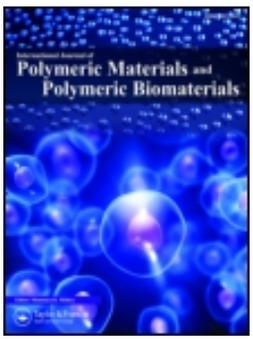

International Journal of Polymeric Materials and Polymeric Biomaterials

ISSN: 0091-4037 (Print) 1563-535X (Online) Journal homepage: http://www.tandfonline.com/loi/gpom20

Development of poly (L-lactide-co-caprolactone) multichannel nerve conduit with aligned electrospun nanofibers for Schwann cell proliferation

M. Aqeel Bhutto, Jianguang Zhang, Binbin Sun, Hany El-Hamshary, Salem S. Al-Deyab & Xiumei Mo

To cite this article: M. Aqeel Bhutto, Jianguang Zhang, Binbin Sun, Hany El-Hamshary, Salem S. Al-Deyab & Xiumei Mo (2016) Development of poly (L-lactide-co-caprolactone) multichannel nerve conduit with aligned electrospun nanofibers for Schwann cell proliferation, International Journal of Polymeric Materials and Polymeric Biomaterials, 65:7, 323-329, DOI: 10.1080/00914037.2015.1099104

To link to this article: http://dx.doi.org/10.1080/00914037.2015.1099104

INTERNATIONAL JOURNAL OF POLYMERIC MATERIALS AND POLYMERIC BIOMATERIALS
2016, VOL. 65, NO. 7, 323–329
http://dx.doi.org/10.1080/00914037.2015.1099104

Taylor & Francis
Taylor & Francis Group

Development of poly (L-lactide-co-caprolactone) multichannel nerve conduit with aligned electrospun nanofibers for Schwann cell proliferation

M. Aqeel Bhutto[a], Jianguang Zhang[a], Binbin Sun[a], Hany El-Hamshary[b,c], Salem S. Al-Deyab[b] and Xiumei Mo[a,b]

[a]Biomaterials and Tissue Engineering Lab, College of Chemistry, Chemical Engineering & Biotechnology, Donghua University, Shanghai, China; [b]Department of Chemistry, College of Science, King Saud University, Riyadh, Saudi Arabia; [c]Department of Chemistry, Faculty of Science, Tanta University, Tanta, Egypt

ABSTRACT

Biomaterials are playing a significant role in understanding and promoting the plasticity and repair of the nervous system. Biomimetic nanofibrous scaffolds mimicking important features of the native extracellular matrix provide a promising strategy to restore functions or achieve favorable responses for tissue regeneration and autograft nerve conduit is one of the most promising nerve regeneration strategies. The present study is based on novel fabrication method by using a special collector for 3D multichannel nerve conduit, longitudinally oriented with aligned electrospun nanofibers. The conduit contained a high number of channels (varying from 7 to 19) and each channel showed a separate morphology. Nerve channels were fabricated with the varying length ranging from 4 to 9 cm and total diameter ranging from 2200 ± 40 µm to 3951 ± 196 µm, while the channel diameter ranging from 350 ± 86 µm to 780 ± 20 µm. It has been clearly shown that the average porosity of nerve conduits has reached almost 89%. In this study, we optimized the parameters to control the structural stability, including the size and the number of channels in the nerve conduit. We also checked *in vitro* cell biocompatibility of multichannel nerve conduit and demonstrated that Schwann cells have the tendency to grow along the direction of nanofibers and high cell growth was observed in high number of channels compared to low number of channels. These results elaborated the potential use of this biocompatible multichannel nerve conduit for further in vivo testing.

GRAPHICAL ABSTRACT

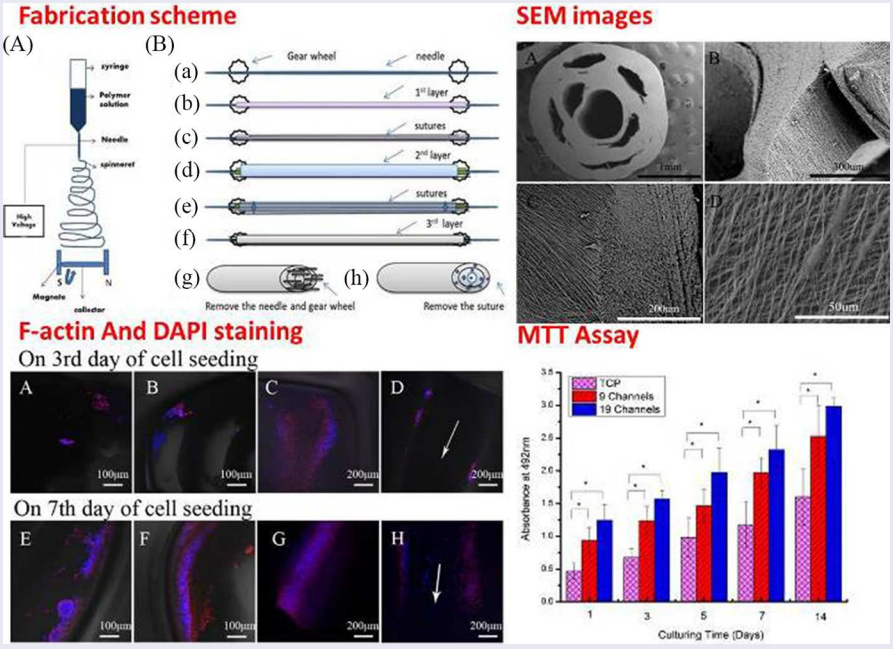

ARTICLE HISTORY
Received 18 May 2015
Accepted 20 September 2015

KEYWORDS
Aligned electrospun nanofibers; electrospinning; multichannel nerve conduit; P(LLA-CL); Schwann cells

1. Introduction

Peripheral nerve injuries are one of the common problems in trauma patients and in those injuries partial or complete loss of nerve function is frequent during surgical reconstruction. Approximately 2.8% nerve injury cases have been reported annually during trauma [1]. In peripheral nerve systems,

CONTACT Xiumei Mo xmm@dhu.edu.cn Biomaterials and Tissue Engineering Lab, College of Chemistry, Chemical Engineering & Biotechnology, Donghua University, Shanghai, 201620 China.
Color versions of one or more of the figures in the article can be found online at www.tandfonline.com/gpom.

regeneration of injured nerve by implanting of autografts or synthetic conduits can be achieved when the length of damaged gap is less than 5 cm [2]. Biomaterial-based conduit is best alternate to substitute the peripheral nerve injuries due to the disadvantages of autografts such as morbidity of donor site, incomplete yield or partial recovery, and difference in size [3,4]. Though commercially available nerve conduits are best for small gaps but not for larger gaps because physical topography or chemical cues are not identical, and so they can recapitulates the hierarchical organization and biological functions of the native nerve [5]. The native nerve is enclosed with an extracellular matrix that is fibrous and porous [6,7]. Nanofibrous scaffolds fabricated by electrospinning provide a suitable environment for cell attachment and proliferation, because of the similar physical dimension as natural extracellular matrix (ECM) [8]. The orientation of electrospun nanofibers plays an important role in cell growth and related functions [9], whereas it is also reported that aligned electrospun fibers have demonstrated utility in directing nerve outgrowth as well as inducing morphological changes [10–13]. Although electrospinning is best for production of two-dimensional meshes, incorporation into three-dimensional constructs for nerve regeneration is difficult and limited [14]. Clinically available nerve grafts are limited to single-lumen conduit constructed of collagen, poly (glycolic acid), poly (D,L-lactide-co-ε-caprolactone), poly(vinyl alcohol), or decellularized ECM, and their recovery is not similar to autografts [15]. Adequate achievements through experiments have been succeeded by nerve autografts and muscle basal lamina [2]. It may be due to in part to the confinement of the nerve within the complex multi-channel structure of the basal lamina [16]. However, researchers have made an effort for various fabrication methods to mimic multichannel structure but fail to succeed same design [17].

Recently, Jeffries and Wang [16] produced a multichannel nerve conduit by using template electrospinning, although this model fulfills the 3D nature of native nerve but thin layer of circumferential aligned fibers is present only on the top of the guide to hold the tube structure while internal structure is consisted of random fibers. To address the previously mentioned challenges, novel fabrication scheme for multichannel nerve conduit has been proposed, which is very simple and entire conduit is made up of only one type of uniform longitudinal aligned electrospun nanofibers. We believe that our proposed model is more supportive in comparison to other models because it contains aligned nanofibers with open porous longitudinal microchannel structures, which promote directional cell growth. Further, *in vitro* testing was performed by using Schwann cells to evaluate the growth rate of cells on present nerve conduit.

2. Experimental

2.1. Material

The copolymer of poly (L-lactide-co-caprolactone) (P(LLA-CL); 50:50) was purchased from Gunze Limited (Japan). Cell culture reagents including fetal bovine serum (FBS), horse serum (HS), Dulbecco's modified Eagle's medium (DMEM), phosphate-buffered saline (PBS), trypsin/EDTA, RPMI 1640 medium, and penicillin–streptomycin were purchased from Gibco BRL, Life Technologies, USA, while the rest of the reagents and chemicals for cell culture and seeding were purchased from Invitrogen and Sigma Aldrich (St. Louis, MO). The mouse Schwann cells for *in vitro* analysis were obtained from the Shanghai Institute of Biochemistry and Cell Biology (SIBCB; CAS, China).

2.2. Electrospinning

The 15% (w/v) polymer solution of P(LLA-CL) (50:50) was prepared by dissolving in 5:1 trifluoroethanol:water solution at room temperature and constantly stirred overnight [18]. The schematic diagram for electrospinning process is shown in Figure 1A, the two magnets were used for both sides of collector to achieve the aligned nanofibers. The distance between the needle and the collector was set to 15 cm while the polymer solution was pumped through 21-gauge needle

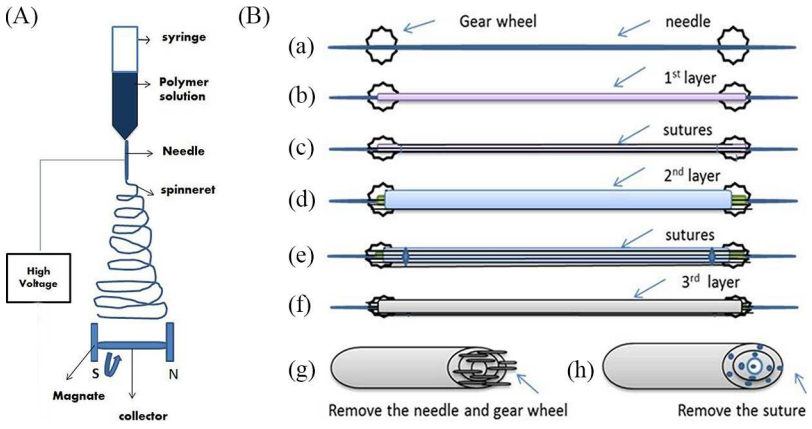

Figure 1. (A) Basic setup of aligned electrospinning. (B) Fabrication scheme for multichannel nerve conduit preparation by multilayer aligned electrospinning. (a) Special collector designed by placing the needle between two small gear wheels. (b) Deposition of first layer on the open surface of collector. (c) Tying up of two aligned sutures over the first layer. (d) Deposition of the second layer of aligned fibers over the sutures. (e) Creation of more channels by again tying more aligned sutures across second layer of polymer solution. (f) Deposition of another layer of aligned fibers on the surface over sutures. (g) Removal of the wheel gear and needle from the nerve conduit. (h) Removal of the sutures manually from nerve conduit.

at a flow rate of 0.8 mL/h. A voltage of 15 kV was generated by a high-voltage power supply and high-power magnets were placed in both side of rotatory collector to produce the aligned fiber, whereas the rotatory collector was used at a speed of 50 rpm for collecting homogenized nanofibers over the collector surface.

2.2.1. Fabrication of multichannel nerve conduit

The schematic diagram of fabrication process is shown in Figure 1A. We have designed the special collector by using the needle and gear wheel (Figure 1B-a) to achieve the multichannel structure in nerve conduit. Briefly, the first layer of nanofibers was deposited on the surface of collector (Figure 1B-b), then two synthetic sutures were regularly fixed on a gear wheel in longitudinal position to produced channels (Figure 1B-c), and a further second layer was deposited on the surface of sutures (Figure 1B-d). Following the these mentioned procedures, four synthetic sutures were used to make channels on second layer and then fabricated one more layer (third layer) to cover the sutures' surface (Figures 1B-e and 1B-f). As a whole, three different layers and six sutures were used to produce the present nerve conduit structure. The total volume of electrospinning solution for each layer was adjusted to 0.8, 1, and 1.2 mL, respectively. The conduit was placed in a vacuum chamber for overnight to remove the residual solvent. After removal of gear wheel, needle and sutures longitudinal multichannel nerve conduit have been formed (Figures 1B-g and 1B-h).The reproducibility and variability of this method was also analyzed by increasing the number of layers and channels in multichannel nerve conduit structure.

2.3. Characterization of multichannel nerve conduit

The structure and surface morphology of the nerve conduit was observed by using a FUJI-Z200 digital camera and scanning electron microscope (SEM; TM-1000, Hitachi, Japan). To maintain the integrity of microchannels, nerve conduits were soaked in deionized water for 1 h and then frozen by ice [16]. The samples were prepared by cutting the nerve conduits into small pieces and dried samples were putter-coated with gold for 10 s twice with the accelerating voltage of 10 kV before the scanning of SEM. On the basis of SEM image, average of the 100 random measurements of diameter distribution, electrospun nanofiber diameters were calculated by using Image J (National Institutes of Health, USA).

2.3.1. Porosity measurement

The porosity of the three nerve conduits were determined by using the method described by Li and Hoffman-Kim [19]. Briefly, the porosity of the nerve conduits includes two parts: the pores in the wall separating the open channels and the channels within the conduit. For the purpose of clarity, V_s, V_c, and V_w were defined as the volume of the whole conduit, channels, and walls, respectively. D and d were the average diameter of the conduit and channels; μ, n, and m were the length of the conduit, the number of channels, and the mass of nerve conduits, respectively. ρ was the density of PLLA-CL, which was 1.25 mg/mm^3. The relationships between these three factors are mentioned in following equations.

$$V_w = V_s - V_c \tag{1}$$

$$V_s = \frac{\pi l}{4} \times D^2 \quad V_c = \frac{n\pi l}{4} \times d^2 \tag{2}$$

$$wall\ porosity(\%) = \left(1 - \frac{m}{V_w \rho}\right) \times 100\% \tag{3}$$

2.4. Cell proliferation and morphology analysis

2.4.1. Cell culturing

Mouse Schwann cells were used for *in vitro* analysis of nerve conduit. The cells were cultured in DMEM containing 10% fetal bovine serum and 1% streptomycin/penicillin and maintained at 37°C with 5% CO_2 incubator. The media were changed on every second day. The nerve conduits were cut into small slices with 1 cm length and placed into 24-well plates. All samples were sterilized by ethanol vaporization for 2 h, and then the samples were washed with sterilized PBS and soaked in cell culture medium. The Schwann cells were pipetted inside the channels of the nerve conduits at the density of 1.0×10^6 cells in total volume for 1 mL per well in a 24-well plate. The plates were placed in low speed shaking incubator at 37°C with 5% CO_2 for 14 days.

2.4.2. MTT assay

The 3-(4,5-dimethylthiazol-2-yl)-2,5-diphenyltetrazolium bromide (MTT; Sigma-Aldrich, USA) assay was used to measure the cell viability and proliferation for 1, 3, 5, 7, and 14 days. Briefly, MTT solution was added to each well, incubated for 4 h at 37°C, and then replaced the dimethyl sulfoxide (DMSO; Sinopharm, China) to dissolve the formazan crystals. The plates were tested at the 492 nm absorbance by using an enzyme-labeled instrument (MK3, Thermo, USA). Each test point has performed three parallel experiments and results of experimental data were calculated by using origin 8.5.T-test was also conducted to find out the silent differences in cell proliferation of different conduits.

2.4.3. F-actin staining with DAPI

For observing the cell invasion and morphology on nerve conduit, after third and seventh days of postseeding with mouse Schwann cells with a density of 1.0×10^6 cells per well, the conduit were washed with PBS to remove the residual medium and unviable cells, and fixed in 4% paraformaldehyde (Thermo Scientific) for 30 min. Fixed samples were rinsed with PBS three times (15 min each time) and blocked in 1% BSA (Sigma) for 30 min. Before staining, the nerve conduit was cut half and sectioned into transverse and longitudinal slices. Subsequently, the cells were labeled with Alexa Fluor 568 Phalloidin (Life Technologies) for 20 minutes and further stain with 4′,6-diamidino-2-phenylindole (DAPI, Vectashield, Vector Laboratories, USA) for 5 min. The mounted samples were observed by laser scanning confocal microscopy (LSCM; Zeiss LSM 700, Germany).

2.4.4. SEM

Cell morphology and interaction between cells and conduits were studied by scanning electron microscope (SEM) at the third day of incubation. The nerve conduits were removed

from culture media and gently washed with PBS as describe before and then fixed with 4% (v/v) paraformaldehyde for 30 min. Further the conduits were dehydrated by using different concentrations of ethanol (30, 50, 70, 90, and 100% (v/v) for 7 min in each concentration and samples were coated with gold and imaged via SEM.

2.5. Statistical analysis

Statical significance of the difference between control and different samples was determined via a paired one-way analysis of variance followed by Bonferroni's multiple comparison test; $p < 0.05$ was considered to be statistically significant.

3. Results and discussion

3.1. Morphology and characterization of multichannel-nerve conduit

The major goal of multichannel conduit construction was to produce endoneurial-like structure with aligned nanofibers in a nerve conduit. The parallel microchannels are present in native nerve and conservation of this endoneurial structure is a positive sign in the prognosis of nerve injuries [20]. The multichannel-nerve conduits were fabricated by making three stable layers of P(LLA-CL) composed of aligned electrospun nanofibers as shown in Figure 2A. The multichannel nerve conduit has seven channels with the total diameter of 2200 ± 40 µm and the average diameter of the core channel and other channels were 780 ± 20 µm and 350 ± 86 µm, respectively. The core channel was bigger in diameter as compared to other channels because of the presence of needle in the center of collector while other channels were formed by the use of synthetic sutures.

We have produced nerve conduits with different length ranging from 4 to 9 cm by using different size collector (Figure 2F). The entire conduits were made up of longitudinally aligned nanofibers as shown in Figures 2B and 2C, which promotes migration of Schwann cells and axon growth. The average diameter of nanofibers was 657 ± 0.15 nm (Figure 2E) and size of the nanofibers can affect interaction between cells and the substrates [21]. Wang et al. [11] reported that Schwann cell proved quickest migration on longitudinally aligned fiber with the diameter ranging from 759 ± 18 nm to 1325 ± 38 nm.

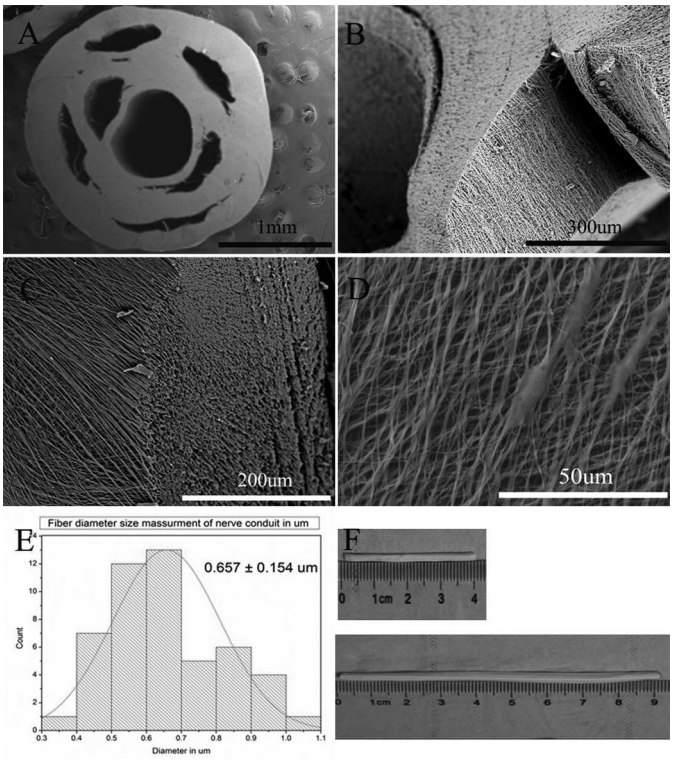

Figure 2. (A) SEM image of multichannel nerve conduit, (B) longitudinal cross section of channel, (C) SEM image of aligned nanofibers, (D) SEM image of Schwann cell morphology: histogram measurement of nanofiber diameter, and (F) digital camera images of different length nerve conduits and surface morphology.

3.2. Reproducibility and variability

Figure 3 shows SEM images of three different nerve conduit structures that vary in diameter, size, and number of channels. The nerve conduit with total diameter of 3178 ± 135 µm and nine channels were fabricated by using three layers of electrospun nanofibers (Figure 3A). The volume for each layer was 0.8, 1.0, and 1.2 mL, respectively. The next nerve conduit (Figure 3B) was fabricated by same way with the volume of 0.8, 1.0, 1.2, 1.4, and 1.5 mL for each layer, respectively, and the average diameter and number of channels increased up to 3951 ± 196 µm and 16, respectively (Figure 3B). Similarly, we fabricated one more conduit by using six layers of same volume of solution as in previous conduit but this time with increased number of sutures and their position. In contrary to previous conduits, we achieved the nerve conduit with high number of channels (19) while no significant change was observed in total diameter (3551 ± 361 µm; Figure 3C) because the approach behind our experiment was to maximize the number of microchannels availability along with sufficient structural stability. It was observed that the channels of upper layer in Figures 3B and 3C were collapsed with the neighboring channel, which effect on the mechanics and shape of channels. These results suggested that we can achieve the high number of channels by increasing number of layers and adjusting sutures position. It was also observed that the channels structure and mechanics can also be controlled by changing volume of electrospun layer.

The synthetic nerve conduit is preferred over the autografts or allografts due to its easy availability and customizability. In this regard, customizability for present nerve conduit can be

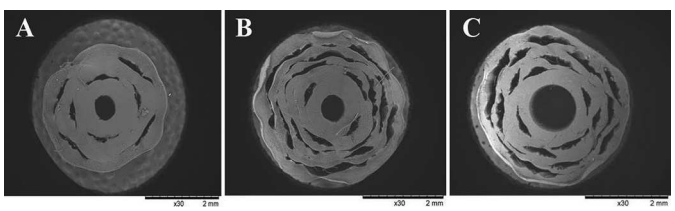

Figure 3. SEM images of multichannel nerve conduit with varying diameter in size and number of channels. (A) nerve conduit having nine channels, (B) nerve conduit having 16 channels, and (C) nerve conduit having 19 channels.

achieved by the changing of electrospinning parameters such as different solvent, concentration of the polymer solution, distance of collector, flow rate and humidity. However, variability can be achieved by changing collector size, thickness, and number of sutures in different layers, while reproducibility can be only maintained by using constant conditions. Three different conduits have been produced by using same electrospinning parameters but different numbers of sutures and layers strategy as shown in Figures 3A–C to demonstrate reproducibility and variability of current method. The time required for nerve conduit construction by using this technique depends on flow rate and the volume of electrospinning solution, while this process took approximately 3–6 h. Nerve conduits showed average porosity of 89% and these results suggested that our nerve conduit is highly porous and helpful in nutrient transportation.

3.3. Comparison with existing methods

Jeffries and Wang have produced multichannel nerve conduit by using two layers of random electrospun nanofibers with template sutures and by rolling of mash tube structure was achieved. The rolling tube was further covered by thin layer of circumferential aligned nanofiber to hold the cylindrical structure [16]. It was found that during the rolling of mesh secondary channels were formed but not continuous structures. However, early degradation of outer layer due to rapid cell growth on aligned fiber could cause the deformation of whole nerve conduit structure. Recently, Dinis et al. [22] also produced the multichannel structure by rolling of aligned electrospun silk mat over the 50 different Teflon sticks. In the previously mentioned model same rolling approach was used but rolling of mat around the different Teflon sticks was very laborious and sensitive work, which directly effects on the reproducibility of results. In comparison to, our method is very simple and nerve conduit does not show any secondary channels structure. It was also observed that smooth surface of the collector allows easy removal from the electrospun fibers without disrupting the conduit structure. In addition no circumferential sheath is required to maintain the cylindrical shape of conduit because highly collaboration of aligned electrospun was observed so no chance of delamination.

Clements et al. [23] produced the nerve conduit structure by inserting the flat sheets of electrospun fibers with cylindrical nerve conduit to fill the lumen while Chew et al. [13] produced the conduit by filling the radially or axially aligned fibers inside the lumen structure. The problem with these conduits is either they do not consume the entire cross-sectional area for adhesion and guidance or not suitably oriented, or their tight filling of bundles may inhibit the Schwann cell migration. In comparison, our nerve conduit provides three-dimensional open channels structure along with uniform aligned electrospun nanofibers. The well-defined multichannel and porous structure facilitates in mass transportation of nutrients and biological agents, whereas multichannel conduits produced by mold casting, lithographic, and deposition techniques have thick or continuous walls that restrict mass transfer [17,24–27]. The versatile features of the current nerve conduit are well channels orientation, size control, and interconnectivity, which make it supreme over other fabrication methods such as freeze drying, thermally induced phase separation, and gas forming methods [28–31].

3.4. Cell morphology and proliferation

Multichannel nerve conduits were cultivated for 14 days under static culture conditions to analyze the proliferation and invasion of cells on conduit, designed for application in peripheral nerve repair. Gu et al. [3] reported that Schwann cells play important role in creating permissive environment during nerve repair through secretion of neurotropic factors, phagocytosis of debris, and deposition of basal lamina, whereas it is still unclear whether Schwann cells lead axonal regeneration [32] or follow axons into a lesion site [33,34]. The Schwann cells have been used from a variety of sources for nerve repair tissue engineering including autologous, allogeneic cell lines, or stem cells because these cells are directly intricate the process of regeneration [3]. Therefore it is important that Schwann cells produce the appropriate response to our nerve conduit structure. The choice of biomaterial and fabrication technique is also an important step in the development of any nerve tube. In our study, we used P(LLA-CL) (50:50) as reported in our previous work that P(LLA-CL) can easily be electrospun and exhibits slow degradation, which is suitable for the regeneration of nerves [10,35]. P(LLA-CL) is a copolymer of L-lactic acid and ε-caprolactone, shown different mechanical properties and biodegradability by changing the weight ratio of lactic acid and ε-caprolactone in the copolymer [6,10].

3.4.1. MTT

To find the effect of multichannel structure on mouse Schwann cell proliferation, the MTT assay was performed (Figure 4) and observed that cells were not only alive but consistently metabolically active until 14 days of culturing. In present experimental model, we have used two different nerve

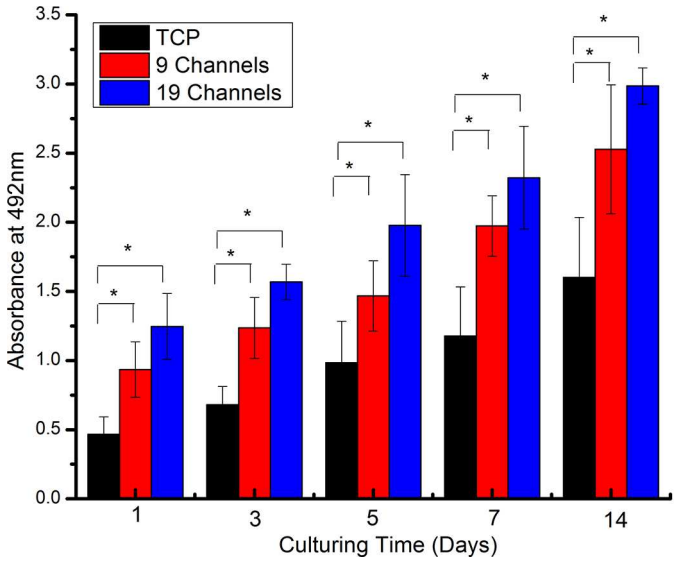

Figure 4. MTT results for seeded nerve conduit, readings were measured in triplicate for each sample (n = 3) and absorbance was read at 492n m (*significantly different in comparison with control, $p < 0.05$, n = 3).

conduit structures that vary in number of channels (nine and 19) to find the effect of number of channels on cell proliferation. Initially both conduits were seeded with the same number of cells and found that 19-channel conduits showed higher cell viability compared to nine-channel conduits because the nerve conduit with a high number of channels provides high surface area for cell attachment compared to that with a low number of channels.

3.4.2. SEM

The morphology of Schwann cells as well as interaction between the cells and conduit fibers were observed by SEM. It was observed that cells adhere to the surface of fiber and extended their cytoplasm along the fiber alignment, which showed longitudinal direction in the nerve conduits (Figure 2D). In addition, cell invasion indicates the porous nature of conduit, which provides enough space and 3D environment for cell growth and migration. It is already reported that aligned nanofibers could provide guidance to form oriented cellular morphologies, which plays an important role in nerve regeneration [36]. In our study, the 3D-aligned scaffolds provided a good microenvironment for Schwann cell proliferation.

3.4.3. F-actin staining with DAPI

We have investigated the distribution pattern of Schwann cells within the nerve conduit structure on third and seventh day of post incubation. The representative confocal laser micrographs of Schwann cells on the conduits showed that Schwann cells spread well on the entire parts of nerve conduit (Figure 5). By assessing results an expansion in cell viability was observed from the third to seventh day. Briefly, Schwann cell migration and proliferation throughout the entire conduit was further supported by increased cell proliferation throughout channels in the transverse-sections of the nerve conduit at the both opening ends (Figures 5A, 5B, 5E, and 5 F). The cells proliferation rate on the upper lamina of the conduits was shown on Figure 5C to Figure 5G from the third to seventh day, respectively. The distribution pattern of cells within the channels were observed low on third day, but drastically improved on seventh day as shown in longitudinal sections of conduit in Figure 5D and Figure 5H, respectively. In present study, cell proliferation and distribution rate may be higher due to directional fiber alignment within the channels whereas, high porosity of electrospun structure and continually low speed shaking also enhances the cells penetration in the channels. Moreover, large open space of present multi-channel structure also offered low growth resistance. Similarly, Kijenska et al. [37] reported the aligned topography of P(LLA-CL) and P(LLA-CL)/collagen I/collagen III nanofibrous scaffolds influenced the behavior of C17.2 cells and higher cell proliferation and differentiation was observed on aligned nanofibers as compared to random nanofibers. However Gupta et al. [38] observed low Schwann cell proliferation on aligned nanofibers of PCL/gelatin nanofibers as compared to random nanofibers. The difference of result is because, they have not used the same size of aligned and random nanofibers scaffolds for Schwann cells proliferation and as we have discussed previously that size of the nanofibers can effect interaction between cells and the substrates [21].

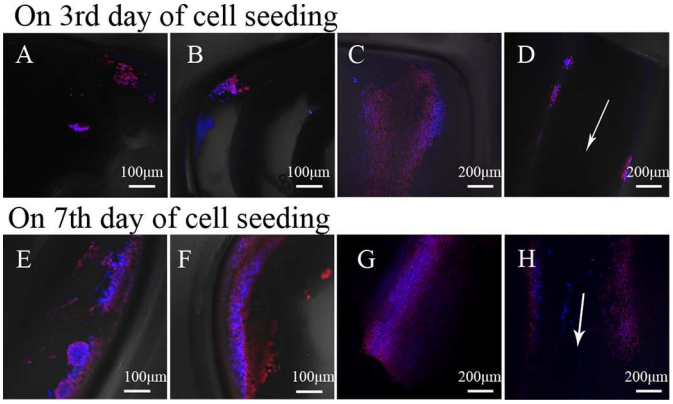

Figure 5. Alexa Fluor 568 Phalloidin with DAPI staining reveals the longitudinal and transverse distribution of Schwann cell nuclei in the multi-channel nerve conduit. (A, B) Transverse section at open end on third day, (C) cell distribution on surface area of nerve conduit on the third day, (D) longitudinal section on the third day, (E, F) transverse section at open end on the seventh day, (G) cells distribution on surface area of nerve conduit on the seventh day, and (H) longitudinal section on the seventh days.

4. Conclusion

In present study, we fabricated the 3D multichannel nerve conduit entirely composed of aligned electrospun fibers with open porous longitudinal microchannels structure. We demonstrated that the high number of channels can be achieved by increasing the number of layers and maximum sutures positioning, while the number of sutures and arrangement should be compared with wall thickness ratio. An *in vitro* study demonstrated that Schwann cells have the tendency to grow along the direction of nanofibers and more cells were observed in high number of channel-nerve conduit compared to low number of channel-nerve conduit. These promising results show potential use of this biocompatible multichannel nerve conduit model for further *in vivo* analysis.

References

[1] Yao, L.; de Ruiter, G. C.; Wang, H.; Knight, A. M.; Spinner, R. J.; Yaszemski, M. J.; Windebank, A. J.; Pandit, A. Controlling dispersion of axonal regeneration using a multichannel collagen nerve conduit. *Biomaterials* **2010**, *31*, 5789–5797.

[2] Schmidt, C. E.; Leach, J. B. Neural tissue engineering: strategies for repair and regeneration. *Annu. Rev. Biomed. Eng.* **2003**, *5*, 293.

[3] Gu, X.; Ding, F.; Yang, Y.; Liu, J. Construction of tissue engineered nerve grafts and their application in peripheral nerve regeneration. *Prog. Neurobiol.* **2010**, *93*, 204–230.

[4] Daly, W.; Yao, L.; Zeugolis, D.; Windebank, A.; Pandit, A. A biomaterials approach to peripheral nerve regeneration: bridging the peripheral nerve gap; and enhancing functional recovery. *J. R. Soc. Interface* **2014**, *9*, 202–221.

[5] Koh, H. S.; Yong, T.; Teo, W. E.; Chan, C. K.; Puhaindran, M. E.; Tan, T. C.; Lim, A.; Lim, B. H.; Ramakrishna, S. In vivo study of novel nanofibrous intra-luminal guidance channels to promote nerve regeneration. *J. Neural Eng.* **2010**, *7*, 046003.

[6] Zhang, K.; Wang, H.; Huang, C.; Su, Y.; Mo, X.; Ikada, Y. Fabrication of silk fibroin blended P(LLA-CL) nanofibrous scaffolds for tissue engineering. *J. Biomed. Mater. Res. A* **2010**, *93*, 984–993.

[7] Biazar, E.; Khorasani, M. T.; Montazeri, N.; Pourshamsian, K.; Daliri, M.; Rezaei, M.; Jabarvand, M.; Khoshzaban, A.; Heidari, S.;

Jafarpour, M. Types of neural conduit and using nanotechnology for peripheral nerve reconstruction. *Int. J. Nanomed.* **2010**, *5*, 839–852.
[8] Chen, Z. G.; Mo, X. M.; He, C. L.; Wang, H. S. *Carbohydr. Polym.* **2008**, *72*, 410–418.
[9] Mauck, R. L.; Baker, B. M.; Nerurkar, N. L.; Burdick, J. A.; Li, W. J.; Tuan, R. S.; Elliott, D. M. Engineering on the straight and narrow: the mechanics of nanofibrous assemblies for fiber-reinforced tissue regeneration. *Tissue Eng. Part B Rev.* **2009**, *15*, 171–193.
[10] Wang, C. Y.; Zhang, K. H.; Fan, C. Y.; Mo, X. M.; Ruan, H. J.; Li, F. F. Aligned natural-synthetic polyblend nanofibers for peripheral nerve regeneration. *Acta Biomater*, **2011**, *7*, 634–643.
[11] Wang, H. B.; Mullins, M. E.; Cregg, J. M.; McCarthy, C. W.; Gilbert, R. J. Varying the diameter of aligned electrospun fibers alters neurite outgrowth and Schwann cell migration *Acta Biomater*. **2010**, *6*, 2970–2978.
[12] Kim, Y. T.; Haftel, V. K.; Kumar, S.; Bellamkonda, R. V. The role of aligned polymer fiber-based constructs in the bridging of long peripheral nerve gaps. *Biomaterials* **2008**, *29*, 3117–3127.
[13] Chew, S. Y.; Mi, R.; Hoke, A.; Leong, K. W. Aligned protein-polymer composite fibers enhance nerve regeneration: a potential tissue-engineering platform. *Adv. Funct. Mater.* **2007**, *17*, 1288–1296.
[14] Jha, B. S.; Colello, R. J.; Bowman, J. R.; Sell, S. A.; Lee, K. D.; Bigbee, J. W.; Bowlin, G. L.; Chow, W. N.; Mathern, B. E.; Simpson, D. G. Two pole air gap electrospinning: Fabrication of highly aligned, three-dimensional scaffolds for nerve reconstruction. *Acta Biomater.* **2011**, *7*, 203–215.
[15] Kehoe, S.; Zhang, X. F.; Boyd, D. FDA approved guidance conduit; and wraps for peripheral nerve injury: a review of materials; and efficacy. *Injury* **2012**, *43*, 553–572.
[16] Jeffries, E. M.; Wang, Y. Biomimetic micropatterned multi-channel nerve conduit by templated electrospinning. *Biotechnol. Bioeng.* **2012**, *109*, 1571–1582.
[17] Yao, L.; Billiar, K. L.; Windebank, A. J.; Pandit, A. Multichanneled collagen conduit for peripheral nerve regeneration: design, fabrication, and characterization. *Tissue Eng. Part C Methods* **2010**, *16*, 1585.
[18] Cao, H.; McHugh, K.; Chew, S. Y.; Anderson, J. M. The topographical effect of electrospun nanofibrous scaffolds on the in vivo and in vitro foreign body reaction. *J. Biomed. Mater. Res. A* **2009**, *93*, 1151–1159.
[19] Li, G. N.; Hoffman-Kim, D. Tissue-engineered platforms of axon guidance. *Tissue Eng. Part B Rev.* **2008**. *14*, 33.
[20] Campbell, W. W. Evaluation and management of peripheral nerve injury. *Clin. Neurophysiol.* **2008**, *119*, 1951–1965.
[21] Agarwal, S.; Wendorff, J. H.; Greiner, A. Use of electrospinning technique for biomedical applications. *Polymer* **2008**, *49*, 5603–5621.
[22] Dinis, T. M.; Elia, R.; Vidal, G.; Dermigny, Q.; Denoeud, C.; Kaplan, D. L.; Egles, C.; Marin, F. 3D multi-channel bi-functionalized silk electrospun conduits for peripheral nerve regeneration. *J. Mech. Behav. Biomed. Mater.* **2015**, *41*, 43–55.
[23] Clements, I. P.; Kim, Y. T.; English, A. W.; Lu, X.; Chung, A.; Bellamkonda, R. V. Thin-film enhanced nerve guidance channels for peripheral nerve repair. *Biomaterials* **2009**, *30*, 3834–3846.
[24] Tran, R. T.; Choy, W. M.; Cao, H.; Qattan, I.; Chiao, J. C.; Ip, W. Y.; Yeung, K. W. K.; Yang, J. Fabrication and characterization of biomimetic multi channeled cross linked-urethane-doped polyester tissue engineered nerve guides. *J. Biomed. Mater. Res. A* **2014**, *102*, 2793–2804.
[25] George, P. M.; Saigal, R.; Lawlor, M. W.; Moore, M. J.; LaVan, D. A.; Marini, R. P.; Selig, M.; Makhni, M.; Burdick, J. A.; Langer, R.; et al. Three-dimensional conductive constructs for nerve regeneration. *J. Biomed. Mater. Res. A* **2009**, *91*, 519–27.
[26] Stokols, S.; Sakamoto, J.; Breckon, C.; Holt, T.; Weiss, J.; Tuszynski, M. H. Templated agarose scaffolds support linear axonal regeneration. *Tissue Eng.* **2006**, *12*, 2777–2787.
[27] Flynn, L.; Dalton, P. D.; Shoichet, M. S. Fiber templating of poly (2-hydroxyethyl methacrylate) for neural tissue engineering. *Biomaterials* **2003**, *24*, 4265–4272.
[28] Bozkurt, A.; Brook, G. A.; Moellers, S.; Lassner, F.; Sellhaus, B.; Weis, J.; Woeltje, M.; Tank, J.; Beckmann, C.; Fuchs, P. In vitro assessment of axonal growth using dorsal root ganglia explants in a novel threedimensional collagen matrix. *Tissue Eng.* **2007**, *13*, 2971–2979.
[29] Hu, X.; Huang, J.; Ye, Z.; Xia, L.; Li, M.; Lv, B.; Shen, X.; Luo, Z. A novel scaffold with longitudinally oriented microchannels promotes peripheral nerve regeneration. *Tissue Eng. Part A* **2009**, *15*, 3297–3308.
[30] Madaghiele, M.; Sannino, A.; Yannas, I. V.; Spector, M. Collagen-based matrices with axially oriented pores. *J. Biomed. Mater. Res. A* **2008**, *85*, 757–767.
[31] Stokols, S.; Tuszynski, M. H. The fabrication and characterization of linearly oriented nerve guidance scaffolds for spinal cord injury. *Biomaterials* **2004**, *25*, 5839–5846.
[32] Chen, Y. Y.; McDonald, D.; Cheng, C.; Magnowski, B.; Durand, J.; Zochodne, D. W. Axon and Schwann cell partnership during nerve regrowth. *J. Neuropathol. Exp. Neurol.* **2005**, *64*, 613–622.
[33] Brushart, T. M. *Nerve Repair*, 1st edn.; Oxford University Press, New York, 2011.
[34] Kettenmann, H.; Ransom, B. R. *Neuroglia*, 2nd edn.; Oxford University Press, New York, 2005.
[35] Zhang, J.; Qiu, K.; Sun, B.; Fang, J.; Zhang, K.; El-Hamshary, H.; Al-Deyab, S. S.; Mo, X. The aligned core–sheath nanofibers with electrical conductivity for neural tissue engineering. *J. Mater. Chem. B* **2014**, *2*, 7945–7954.
[36] Xie, J.; MacEwan, M. R.; Willerth, S. M.; Li, X.; Moran, D. W.; Sakiyama-Elbert, S. E.; Xia, Y. *Adv. Funct. Mater.* **2009**, *19*, 2313–2318.
[37] Kijenska, E.; Prabhakaran, M. P.; Swieszkowski, W.; Kurzydlowski, K. J.; Ramakrishna, S. Electrospun bio-composite P(LLA-CL)/collagen I/collagen III scaffolds for nerve tissue engineering. *J. Biomed. Mater. Res. B* **2012**, *4*, 1093–1102.
[38] Deepika, G.; Venugopal, J.; Prabhakaran, M. P.; Giri Dev, V. R.; Low, L.; Choon, A. T.; Ramakrishna, S. Aligned and random nanofibrous substrate for the in vitro culture of Schwann cells for neural tissue engineering. *Acta Biomater.* **2009**, *5*, 2560–2569.